Appearance of neointima according to stent type and restenotic phase: analysis by optical coherence tomography

Kenji Goto[1]*, MD; Hideo Takebayashi[1], MD, PhD; Yasuki Kihara[2], MD, PhD; Arata Hagikura[1], MD; Yasukazu Fujiwara[1], MD; Yuetsu Kikuta[1], MD; Katsumasa Sato[1], MD; Sunao Kodama[1], MD; Masahito Taniguchi[1], MD; Shigeki Hiramatsu[1], MD, PhD; Seiichi Haruta[1], MD

1. Fukuyama Cardiovascular Hospital, Fukuyama, Japan; 2. Hiroshima University Graduate School of Biomedical Science, Hiroshima, Japan

KEYWORDS

- bare metal stent
- drug-eluting stent
- in-stent restenosis
- neointima
- optical coherence tomography

Abstract

Aims: The features of neointima after bare metal stent (BMS) or drug-eluting stent (DES) implantation have not yet been fully characterised. The aim of this study was to investigate in-stent neointima characteristics according to stent type and restenotic phase.

Methods and results: The study included 59 consecutive patients undergoing target lesion revascularisation for in-stent restenosis (ISR) evaluated by optical coherence tomography (OCT) during the early phase (≤1 year, n=30) and late phase (>1 year, n=29) after either BMS (n=37) or DES (n=22) implantation. The OCT signal patterns of tissues at the minimal lumen area were categorised into three patterns: (1) homogeneous high-signal band, (2) heterogeneous mixed-signal band, and (3) lipid-laden intima. The predominant OCT pattern was homogeneous high-signal band in the BMS early phase (19/21 [91%]), lipid-laden intima in the BMS late phase (12/16 [76%]), and heterogeneous mixed-signal band in the DES late phase (9/13 [69%]). Heterogeneous mixed-signal band was seen more frequently in the DES early phase compared with BMS early phase (44% vs. 9%, p<0.05).

Conclusions: There were differences of neointima according to stent type and restenotic phase, and this may lead to a better understanding of the different mechanisms of ISR.

Corresponding author: Fukuyama Cardiovascular Hospital, 2-39 Midorimachi, Fukuyama, Hiroshima, 720-0804, Japan. E-mail: kgoto0369@yahoo.co.jp

Introduction

Previous studies demonstrated that neointima after bare metal stent (BMS) implantation is mainly composed of vascular smooth muscle cells associated with the vascular healing response in the early phase[1]. However, neointimal tissue inside the stent often transforms into lipid-laden tissue over an extended time period after implantation[2,3]. It is still unknown if neointima morphology associated with in-stent restenosis (ISR) is similar after drug-eluting stent (DES) and BMS implantation. Optical coherence tomography (OCT) is a high-resolution imaging modality capable of investigating detailed vascular healing after stent implantation *in vivo*[4-6]. The aim of this study was to use OCT to compare the morphologic characteristics of neointima between the two stent types (BMS vs. DES) in both the early and late restenotic phases.

Methods

The study population was recruited from 74 consecutive patients who were admitted to Fukuyama Cardiovascular Hospital between April 2009 and August 2011 for target lesion revascularisation (TLR). The ISR lesion that needed TLR was defined as 90% diameter stenosis by visual assessment or 75% to 90% diameter stenosis with myocardial ischaemia. Patients were not eligible for enrolment if they underwent intervention in the setting of primary or emergent percutaneous coronary intervention (PCI) for acute coronary syndrome (ACS) (n=5), had edge restenosis (n=6) or had total occlusion (n=4). The final study population (n=59, 59 lesions) evaluated by OCT included 30 segments in the early phase (≤1 year) and 29 segments in the late phase (>1 year) after implantation of a BMS (n=37) or DES (n=22). The study protocol was approved by the institutional ethics committee of Fukuyama Cardiovascular Hospital, and written consent was obtained from all patients before the procedure.

All lesions responsible for ISR were evaluated by OCT prior to revascularisation. The region of interest included the stent region, but did not include the margins, defined as the stent edges and vessel segments 5 mm proximal or distal to the stent. OCT acquisition was performed using a commercially available system for intracoronary imaging (LightLab Imaging Inc., Westford, MA, USA). A 0.016 inch wire-type imaging catheter (ImagingWire; LightLab Imaging Inc.) was advanced to the distal end of the stent through a 4 Fr over-the-wire occlusion balloon catheter (Helios™; LightLab Imaging). The occlusion balloon was then inflated to 0.3 to 0.5 atm, while lactated Ringer's solution was infused from the balloon tip at 0.5 ml/s to flush blood from the imaging field. The entire stent was imaged with an automatic pullback device moving at 1.5 mm/s.

The two observers were blinded to the clinical and procedural characteristics. Offline analysis was performed with the proprietary LightLab software (LightLab Imaging Inc.). To test the interobserver variability of the OCT ISR patterns, the minimal lumen area (MLA) image was analysed independently by two observers not involved in the primary data analysis. One of the observers repeated the analysis one week later to assess the intraobserver variability.

Cross-sectional images were analysed at longitudinal intervals of 1 mm, and the neointimal area for each cross-section was measured by a method of multiple-pointed trace. The OCT signal patterns of tissues in the region of MLA were categorised into three patterns by agreement of two observers: (1) homogeneous high-signal band, (2) heterogeneous mixed-signal band and (3) lipid-laden intima **(Figure 1)**. A two-layer appearance with visible stent strut was categorised into homogeneous high-signal band, while a two-layer appearance without visible stent struts was categorised into heterogeneous mixed-signal band **(Figure 1B** and **Figure 1C)**. To describe the morphologic appearance of the restenotic tissue, the parameters, including the presence of thin-cap fibroatheroma (TCFA), microvessels, intimal disruption and presence of thrombus, were analysed within the stent **(Figure 2)**. Thrombus was identified as a mass that protruded into the vessel lumen from the surface of the vessel wall[7,8]. Red thrombus was defined as high-backscattering protrusions inside the lumen of the artery with signal-free shadowing in the OCT image **(Figure 2E)**. White thrombus was defined as signal-rich with low-backscattering protrusions **(Figure 2F)**. Lipid-laden intima was defined as a signal-poor region with diffuse borders. Calcification was defined as well-delineated, signal-poor mass with a sharp border[9]. For all plaques with an OCT-determined lipid core, the fibrous cap thickness was measured at its thinnest part. If the fibrous cap of a given plaque was visible, cap thicknesses were measured five times and the average of the three middle values was calculated. A TCFA was defined by OCT analysis as a plaque with lipid content in ≥1 quadrant and the thinnest part of a fibrous cap measuring ≤65 μm.

The restenotic tissue area was defined as the stent area minus the lumen area. Restenotic tissue burden was defined as restenotic tissue area/stent area ×100. The cross-section containing the MLA was used to determine the maximum and the minimum restenotic tissue thickness and to calculate the restenotic tissue symmetry ratio (maximum restenotic tissue thickness/maximum restenotic tissue thickness − minimum restenotic tissue thickness)[10]. OCT restenosis length was defined as the lesion length with >50% cross-sectional area narrowing by neointimal formation. A lesion <10 mm was defined as a focal lesion. When the strut was not fully visible, the position of the stent strut was measured according to the proximal and distal visible struts with longitudinal findings.

We compared the data as follows: (1) within the same stent types (BMS or DES) to compare the early phase with the late phase; (2) within the same phase to compare the different stents (BMS vs. DES). Data are expressed as mean±SD for continuous variables and as percentages for categorical variables. Continuous variables were compared using a Student's t-test. Categorical variables were compared using a chi-square test or Fisher's exact test, as appropriate. Kappa (κ) test was used to assess the interobserver and intraobserver variability for qualitative OCT assessment. All calculated p-values were two-sided and differences were considered to be statistically significant when the respective p-values were <0.05.

Results

Baseline clinical characteristics according to stent type and restenotic phase are shown in **Table 1**. Patient characteristics were not significantly different among the four groups. Stents were implanted
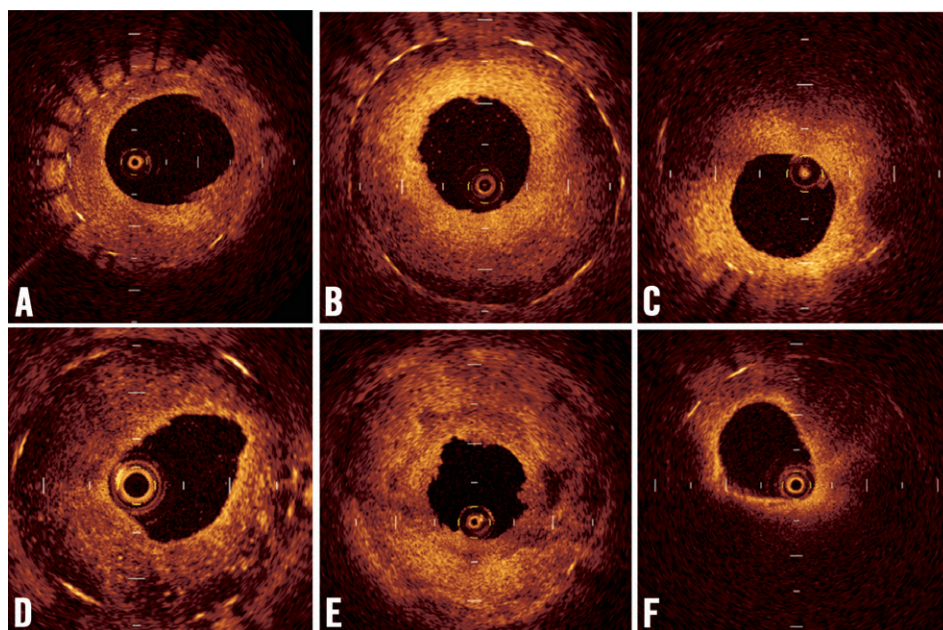
Figure 1. *Patterns of neointima at minimum stent area by optical coherence tomography. The neointima was classified into the following categories: (A) homogeneous high-signal band, (B) homogeneous high-signal band which has a two-layer appearance with visible stent struts, (C) heterogeneous mixed-signal band which has a two-layer appearance without visible stent struts, (D) heterogeneous mixed-signal band with a speckled pattern, (E) heterogeneous mixed-signal band with low and high backscatter, and (F) lipid-laden intima (sudden attenuated intima with diffuse borders).*

originally for stable angina in 33 (56%), ACS in 24 (41%) and chronic total occlusion in two (4%) of the cases. A BMS was implanted more frequently than a DES in ACS patients (57% vs. 14%, respectively, p=0.001). There were no significant differences among the four groups concerning the location of the target lesion or medications used at the time of TLR.

Although the mean duration from stent implantation to OCT was similar between the BMS early phase and DES early phase

Table 1. Baseline characteristics.

| | | BMS | | | DES | | | | |
		Early phase (n=21)	Late phase (n=16)	*p*-value*	Early phase (n=9)	Late phase (n=13)	*p*-value**	*p*-value¶	*p*-value¶¶
Demographics	Age, yr	67±9	68±7	0.59	60±11	66±10	0.27	0.10	0.36
	Male	20 (95%)	15 (94%)	>0.99	8 (89%)	9 (69%)	0.36	0.52	0.14
	Hypertension	16 (76%)	14 (88%)	0.67	6 (67%)	11 (85%)	0.61	0.67	>0.99
	Hyperlipidaemia	13 (62%)	11 (69%)	0.93	7 (78%)	9 (69%)	>0.99	0.67	>0.99
	Diabetes	5 (24%)	9 (56%)	0.09	5 (56%)	8 (62%)	>0.99	0.12	>0.99
	Smoking	9 (43%)	6 (38%)	>0.99	3 (33%)	9 (69%)	0.22	0.70	0.18
Clinical presentation at the index PCI	ACS	11 (52%)	10 (63%)	0.77	1 (11%)	2 (15%)	0.49	<0.05	0.03
	AP	9 (43%)	6 (38%)	>0.99	8 (89%)	10 (77%)	0.62	0.04	0.08
	CTO	1 (5%)	0	>0.99	0	1 (8%)	>0.99	0.99	0.45
Vessel	left anterior descending artery	11 (52%)	10 (63%)	0.77	4 (44%)	8 (62%)	0.67	>0.99	>0.99
	left circumflex artery	1 (5%)	2 (13%)	0.57	1 (11%)	2 (15%)	>0.99	0.52	>0.99
	right coronary artery	9 (43%)	8 (50%)	0.91	4 (44%)	3 (23%)	0.38	>0.99	0.25
Medications at TLR	Statins	16 (76%)	12 (75%)	>0.99	7 (78%)	11 (85%)	>0.99	>0.99	0.66
	Aspirin	21 (100%)	16 (100%)	>0.99	9 (100%)	13 (100%)	>0.99	>0.99	>0.99
	Thienopyridine	18 (86%)	13 (81%)	>0.99	9 (100%)	12 (92%)	>0.99	0.53	0.61

ACS: acute coronary syndrome; AP: angina pectoris; BMS: bare metal stent; CTO: chronic total occlusion; DES: drug-eluting stent; PCI: percutaneous coronary intervention; TLR: target lesion revascularisation; *p*-value*: early phase vs. late phase in BMS; *p*-value**: early phase vs. late phase in DES; *p*-value¶: BMS vs. DES in early phase; *p*-value¶¶: BMS vs. DES in late phase
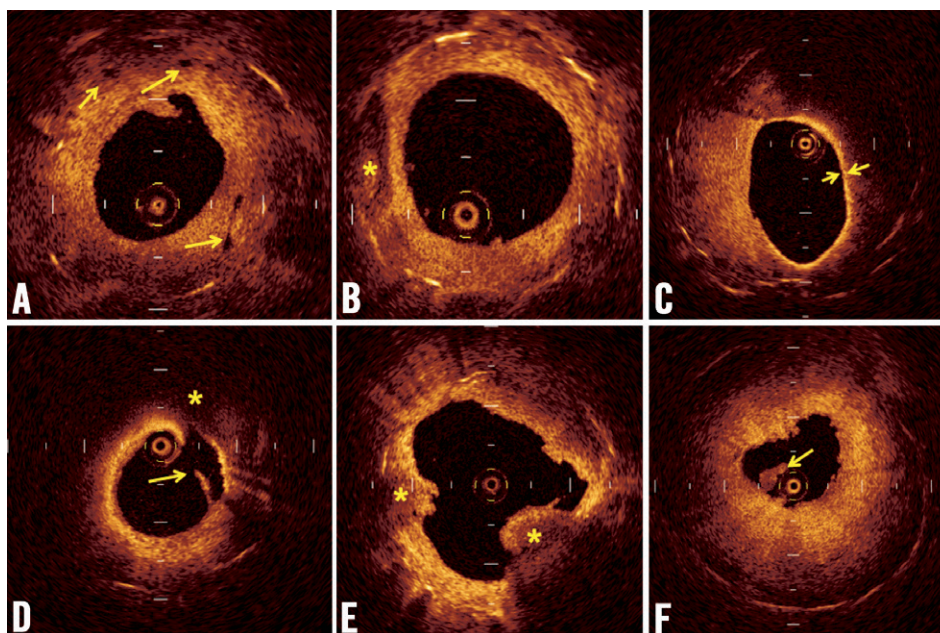
Figure 2. *Representative findings of in-stent neointima by optical coherence tomography. (A) Microvessels appear as well-delineated, low-backscattering structures less than 200 microns in diameter. (B) Calcification was defined as a well-delineated, signal-poor mass with sharp borders. (C) A thin-cap fibroatheroma (TCFA) was defined as a plaque with lipid content in ≥1 quadrant and the thinnest part of a fibrous cap measuring ≤65 μm. (D) Disrupted intima (yellow arrow) and lipid tissue (*) are seen. (E) Red thrombus (*) is high-backscattering protrusion with signal-free shadow. (F) White thrombus (yellow arrow) was characterised as signal-rich and low-backscattering protrusion.*

(218±51 days vs. 207±67 days, respectively, p=0.63), the duration was significantly longer in the BMS late phase compared with the DES late phase (3,014±1,260 days vs. 1,021±535 days, respectively, p<0.0001). Stent size was significantly greater and stent length tended to be shorter in the two BMS groups compared with the two DES groups. Among nine ISR segments in the DES early phase, there were two sirolimus-eluting stents (SESs), two paclitaxel-eluting stents (PESs) and five everolimus-eluting stents (EESs). In contrast, among 13 ISR segments in the DES late phase, there were six SESs, six PESs, and one EES **(Table 2)**.

Homogeneous high-signal band was found in 19 (91%) of 21 cases in the BMS early phase, and lipid-laden intima was seen in 12 (75%) of 16 patients in the BMS late phase. The predominant findings were heterogeneous mixed-signal band (69%); while the rate of lipid-laden intima was rare (8%) in DES late phase **(Table 3)**. Heterogeneous mixed-signal band was more frequently seen in DES compared with BMS in the early phase (44% vs. 9%, p<0.05). Although the prevalence of intracoronary thrombus was not rare (n=11, 19%) in this stable angina population, the majority of the thrombus was white thrombus (n=8, 73%), except for three cases of red thrombus in BMS late phase. Intimal disruption was seen more frequently in BMS late phase than in BMS early phase (50% vs. 10%, p=0.001). Of note, the thrombus was more frequently observed in patients with intimal disruption than those without it (54% [7/13] vs. 9% [4/46], p=0.001) and in those with lipid-laden intima than those without it (38% [5/13] vs. 13% [6/46], p=0.05).

Table 2. Stent information.

		BMS			DES				
		Early phase (n=21)	Late phase (n=16)	*p*-value*	Early phase (n=9)	Late phase (n=13)	*p*-value**	*p*-value¶	*p*-value¶¶
Time from stent implantation, days		218±51	3,014±1,260	<0.0001	207±67	1,021±535	0.0002	0.63	<0.0001
Stent size, mm		3.4±0.4	3.3±0.5	0.32	2.9±0.3	2.9±0.4	0.90	0.003	0.06
Stent length, mm		21.0±8.7	16.8±5.8	0.11	22.7±6.6	25.3±16.1	0.65	0.60	0.06
DES type	– Sirolimus	n/a	n/a	n/a	2 (22%)	6 (46%)	0.38	n/a	n/a
	– Paclitaxel	n/a	n/a	n/a	2 (22%)	6 (46%)	0.38	n/a	n/a
	– Everolimus	n/a	n/a	n/a	5 (56%)	1 (8%)	0.38	n/a	n/a

BMS: bare metal stent; DES: drug-eluting stent; *p*-value*: early phase vs. late phase in BMS; *p*-value**: early phase vs. late phase in DES; *p*-value¶: BMS vs. DES in early phase; *p*-value¶¶: BMS vs. DES in late phase

Table 3. Optical coherence tomography.

	BMS			DES				
	Early phase (n=21)	Late phase (n=16)	*p*-value*	Early phase (n=9)	Late phase (n=13)	*p*-value**	*p*-value¶	*p*-value¶¶
Qualitative assessment								
Tissue coverage structure								
Homogeneous high-signal band	19 (91%)	2 (12%)	<0.0001	5 (56%)	3 (23%)	0.08	0.14	0.63
Heterogeneous mixed-signal band	2 (9%)	2 (12%)	>0.99	4 (44%)	9 (69%)	0.19	<0.05	0.003
Lipid-laden intima	0	12 (76%)	<0.0001	0	1 (8%)	>0.99	>0.99	0.001
Thrombus	3 (14%)	6 (38%)	0.14	1 (11%)	1 (8%)	>0.99	>0.99	0.09
Red thrombus	0	3 (19%)	0.46	0	0	>0.99	>0.99	>0.99
White thrombus	3 (14%)	3 (19%)	n/a	1 (11%)	1 (8%)	n/a	n/a	n/a
Microvessels	16 (76%)	13 (81%)	>0.99	6 (67%)	8 (62%)	0.66	>0.99	0.41
Intimal disruption	2 (10%)	8 (50%)	0.001	0	3 (23%)	0.24	>0.99	0.25
Calcification	0	5 (31%)	0.01	0	0	>0.99	>0.99	<0.05
Quantitative assessment								
Mean stent area, mm^2	9.2±2.3	9.0±2.8	0.78	7.1±2.6	6.8±1.8	0.79	0.03	0.02
Mean lumen area, mm^2	1.3±0.4	1.4±0.4	0.89	1.4±0.5	1.2±0.5	0.34	0.95	0.34
Mean restenotic tissue area, mm^2	7.9±2.2	7.6±2.7	0.73	5.7±2.6	5.7±1.7	0.95	0.03	0.03
Intimal area, %	84.9±5.1	84.1±4.9	0.65	78.5±9.9	82.2±7.0	0.32	0.03	0.39
Restenosis length, mm	10.2±7.0	6.0±2.6	0.03	5.4±2.0	5.3±2.7	0.98	0.05	0.50
Neointima symmetry ratio	2.0±0.5	3.0±2.3	0.06	2.4±1.1	3.1±2.7	0.46	0.17	0.89
Focal restenosis	9 (43%)	8 (50%)	0.91	9 (100%)	11 (85%)	0.49	0.004	0.11

BMS: bare metal stent; DES: drug-eluting stent; *p*-value*: early phase vs. late phase in BMS; *p*-value**: early phase vs. late phase in DES; *p*-value¶: BMS vs. DES in early phase; *p*-value¶¶: BMS vs. DES in late phase

A TCFA was seen in two (18%) of the 11 patients with lipid-laden intima in the BMS late phase. The reproducibility variability for the in-stent restenosis OCT signal patterns was as follows; κ=0.84 for interobserver and κ=0.94 for intraobserver.

The stent areas at the site of MLA and restenotic tissue area were significantly different among the four groups, whereas the MLA and % intimal area were similar among the four groups. Lesion length was significantly longer in the two BMS groups compared with the two DES groups.

Discussion

In a previous study, tissue coverage appearance was categorised into three types: layered, homogeneous, and heterogeneous[6]. In other studies, the layered pattern was classified into two patterns, including two-layer with visible struts and two-layer without visible struts, because OCT signal patterns in DES ISR were more varied than in BMS ISR[11,12]. In the current study, the layered pattern was classified into two patterns according to the predominance of the low-backscatter area. A two-layer appearance with visible stent struts was categorised as homogeneous high-signal band **(Figure 1B)**, while a two-layer appearance without visible stent struts was categorised as heterogeneous mixed-signal band **(Figure 1C)**. A previous pathology study demonstrated that OCT images of fibrous plaques were characterised by homogeneous, signal-rich regions, fibrocalcific plaques by well-delineated, signal-poor regions with sharp borders, and lipid-rich plaques by signal-poor regions with diffuse borders. However, a predominantly fibrous plaque containing small amounts of lipid could be misdiagnosed as lipid-rich plaque[9]. In the future, further study is warranted to compare the OCT two-layer findings and histologic tissue components. However, of note, the restenotic tissue structure could be assessed by *in vivo* OCT with low interobserver and intraobserver variability.

The heterogeneous mixed-signal band which included low-backscatter signal was more frequently observed in DES than in BMS in the early phase. Previous studies demonstrated that low-signal images in the deep tissue layer suggest fibrin surrounded by proteoglycan extracellular matrix[13,14]. Therefore, the heterogeneous low-intensity areas in the DES seemed to represent delayed arterial healing, possibly resulting from peri-strut inflammation. These findings could be consistent with previous studies that demonstrated DES showed an earlier onset of neoatherosclerosis and a higher incidence of lesion formation as compared with BMS[15]. On the other hand, our data demonstrated that the neointima of the BMS early phase was homogeneous high-signal band, which is mainly composed of vascular smooth muscle cells[1,16]. The neointima of the BMS late phase was lipid-laden intima, which is similar to that of so-called "*de novo* atherosclerosis". These findings could be consistent with previous studies that demonstrated stable fibrous neointima changed into lipid-rich plaque five years after BMS implantation[2,3,17].

Intraluminal thrombus was seen in 11 (19%) of 59 patients in this stable angina population. The majority of the thrombus was white thrombus, which is considered an older thrombus in the process of thrombus organisation and mainly consists of platelet and fibrin[7]. Pathologic studies have demonstrated that organised thrombus can be a component of restenosis in both BMS and DES[18-20]. On the other hand, plaque rupture with subsequent thrombus formation is the most frequent cause of acute coronary syndromes, such as acute myocardial infarction[21]. In the current study, thrombus was more frequently seen in the patients with intimal disruption or lipid-laden intima compared to those without them. These findings are consistent with the previous studies which demonstrated that thrombus formation was closely associated with intimal disruption and lipid-laden intima[2,22]. Although it was not clear why some intracoronary thrombus culminated in ACS and some did not, angiographic evidence of complexity does not by itself necessarily determine the destiny of a plaque[23]. In other words, although angiographically determined complexity correlates closely with plaque instability pathologically, such plaques may remain stable over time[24,25].

Previous OCT studies were not completely consistent with regard to the prevalence of plaque rupture, red thrombus and/or lipid-laden intima[2,12,26,27]. A possible explanation for these differences may be the variability of factors including the time after stent implantation, stent type, intimal burden, and different disease acuity (unstable or stable angina).

Study limitations

The present study has several limitations. First, this was a single-centre study based on a relatively limited sample size, raising the possibility of selection bias. In addition, no comparison among DES types could be performed due to the limited number. The study should be considered only exploratory. Second, the diagnosis at the index PCI was significantly different between the patients with BMS and DES implantation. Third, we cannot simply compare the difference between the intima of the BMS late phase and DES late phase, because the average time interval between initial stent implantation and OCT imaging was significantly longer in the BMS late phase compared with the DES late phase. Finally, the main limitation is the lack of histologic data to validate the OCT findings.

Conclusion

The present OCT study demonstrated different characteristics of neointima based on stent type and restenotic phase. The predominant findings of neointima were homogeneous high-signal band in the BMS early phase, lipid-laden intima in the BMS late phase, and heterogeneous mixed-signal band in the DES late phase. Heterogeneous mixed-signal band was seen more frequently in DES compared with BMS in the early phase (44% vs. 9%, p<0.05). The present study suggests that the vascular healing pattern was somewhat different according to stent type and restenotic phase, and these findings may help to explain the different mechanisms of ISR.

Conflict of interest statement

The authors have no conflicts of interest to declare.

References

1. Grewe PH, Deneke T, Machraoui A, Barmeyer J, Müller KM. Acute and chronic tissue response to coronary stent implantation: pathologic findings in human specimen. *J Am Coll Cardiol.* 2000;35:157-63.

2. Takano M, Yamamoto M, Inami S, Murakami D, Ohba T, Seino Y, Mizuno K. Appearance of lipid-laden intima and neovascularization after implantation of bare-metal stents. Extended late-phase observation by intracoronary optical coherence tomography. *J Am Coll Cardiol.* 2010;55:26-32.

3. Hasegawa K, Tamai H, Kyo E, Kosuga K, Ikeguchi S, Hata T, Okada M, Fujita S, Tsuji T, Takeda S, Fukuhara R, Kikuta Y, Motohara S, Ono K, Takeuchi E. Histopathological findings of new in-stent lesions developed beyond five years. *Catheter Cardiovasc Interv.* 2006;68:554-8.

4. Jang IK, Bouma BE, Kang DH, Park SJ, Park SW, Seung KB, Choi KB, Shishkov M, Schlendorf K, Pomerantsev E, Houser SL, Aretz HT, Tearney GJ. Visualization of coronary atherosclerotic plaques in patients using optical coherence tomography: comparison with intravascular ultrasound. *J Am Coll Cardiol.* 2002;39:604-9.

5. Yamaguchi T, Terashima M, Akasaka T, Hayashi T, Mizuno K, Muramatsu T, Nakamura M, Nakamura S, Saito S, Takano M, Takayama T, Yoshikawa J, Suzuki T. Safety and feasibility of an intravascular optical coherence tomography image wire system in the clinical setting. *Am J Cardiol.* 2008;101:562-7.

6. Gonzalo N, Serruys PW, Okamura T, van Beusekom HM, Garcia-Garcia HM, van Soest G, van der Giessen W, Regar E. Optical coherence tomography patterns of stent restenosis. *Am Heart J.* 2009;158:284-93.

7. Takano M, Inami S, Ishibashi F, Okamatsu K, Seimiya K, Ohba T, Sakai S, Mizuno K. Angioscopic follow-up study of coronary ruptured plaques in nonculprit lesions. *J Am Coll Cardiol.* 2005;45:652-8.

8. Kume T, Akasaka T, Kawamoto T, Watanabe N, Toyota E, Neishi Y, Sukmawan R, Sadahira Y, Yoshida K. Assessment of coronary arterial thrombus by optical coherence tomography. *Am J Cardiol.* 2006;97:1713-7.

9. Yabushita H, Bouma BE, Houser SL, Aretz HT, Jang IK, Schlendorf KH, Kauffman CR, Shishkov M, Kang DH, Halpern EF, Tearney GJ. Characterization of human atherosclerosis by optical coherence tomography. *Circulation.* 2002;106:1640-5.

10. Gonzalo N, Barlis P, Serruys PW, Garcia-Garcia HM, Onuma Y, Ligthart J, Regar E. Incomplete stent apposition and delayed tissue coverage are more frequent in drug eluting stents implanted during primary percutaneous coronary intervention for ST-elevation myocardial infarction than in drug eluting stents implanted for stable/unstable angina: insights from optical coherence tomography. *JACC Cardiovasc Interv.* 2009;2:445-52.

11. Yamamoto M, Takano M, Murakami D, Inami T, Kimata N, Inami S, Okamatsu K, Ohba T, Seino Y, Mizuno K. Optical coher-

ence tomography analysis for restenosis of drug-eluting stents. *Int J Cardiol.* 2011;146:100-3.

12. Kang SJ, Mintz GS, Akasaka T, Park DW, Lee JY, Kim WJ, Lee SW, Kim YH, Whan Lee C, Park SW, Park SJ. Optical coherence tomographic analysis of in-stent neoatherosclerosis after drug-eluting stent implantation. *Circulation.* 2011;123:2954-63.

13. Teramoto T, Ikeno F, Otake H, Lyons JK, van Beusekom HM, Fearon WF, Yeung AC. Intriguing peri-strut low-intensity area detected by optical coherence tomography after coronary stent deployment. *Circ J.* 2010;74:1257-9.

14. Kume T, Okura H, Kawamoto T, Akasaka T, Toyota E, Watanabe N, Neishi Y, Sadahira Y, Yoshida K. Fibrin clot visualized by optical coherence tomography. *Circulation.* 2008;118:426-7.

15. Nakazawa G, Otsuka F, Nakano M, Vorpahl M, Yazdani SK, Ladich E, Kolodgie FD, Finn AV, Virmani R. The pathology of neoatherosclerosis in human coronary implants bare-metal and drug-eluting stents. *J Am Coll Cardiol.* 2011;57:1314-22.

16. Ramcharitar S, Garcia-Garcia HM, Nakazawa G, Kukreja N, Ligthart J, Virmani R, Serruys PW. Ultrasonic and pathological evidence of a neo-intimal plaque rupture in patients with bare metal stents. *EuroIntervention.* 2007;3:290-1.

17. Inoue K, Abe K, Ando K, Shirai S, Nishiyama K, Nakanishi M, Yamada T, Sakai K, Nakagawa Y, Hamasaki N, Kimura T, Nobuyoshi M, Miyamoto TA. Pathological analyses of long-term intracoronary Palmaz-Schatz stenting; Is its efficacy permanent? *Cardiovasc Pathol.* 2004;13:109-15.

18. van Beusekom HM, Saia F, Zindler JD, Lemos PA, Swager-Ten Hoor SL, van Leeuwen MA, de Feijter PJ, Serruys PW, van der Giessen WJ. Drug-eluting stents show delayed healing: paclitaxel more pronounced than sirolimus. *Eur Heart J.* 2007;28:974-9.

19. Komatsu R, Ueda M, Naruko T, Kojima A, Becker AE. Neointimal tissue response at sites of coronary stenting in humans: macroscopic, histological, and immunohistochemical analyses. *Circulation.* 1998;98:224-33.

20. Glover C, Ma X, Chen YX, Miller H, Veinot J, Labinaz M, O'Brien E. Human in-stent restenosis tissue obtained by means of coronary atherectomy consists of an abundant proteoglycan matrix with a paucity of cell proliferation. *Am Heart J.* 2002;144:702-9.

21. Davies M, Thomas A. Thrombosis and acute coronary artery lesions in sudden cardiac ischemic death. *N Engl J Med.* 1984;310:1137-40.

22. Jang IK, Tearney GJ, MacNeill, Takano M, Moselewski F, Iftima N, Shishkov M, Houser S, Aretz HT, Halpern EF, Bouma BE. In vivo characterization of coronary atherosclerotic plaque by use of optical coherence tomography. *Circulation.* 2005;111:1551-5.

23. Haft JI, al-Zarka AM. The origin and fate of complex coronary lesions. *Am Heart J.* 1991;121:1050-61.

24. Haft JI, al-Zarka AM. Comparison of the natural history of irregular and smooth coronary lesions: insights into the pathogenesis, progression, and prognosis of coronary atherosclerosis. *Am Heart J.* 1993;126:551-61.

25. Levin DC, Fallon JT. Significance of the angiographic morphology of localized coronary stenoses: histopathologic correlations. *Circulation.* 1982;66:316-20.

26. Kashiwagi M, Kitabata H, Tanaka A, Okochi K, Ishibashi K, Komukai K, Tanimoto T, Ino Y, Takarada S, Kubo T, Hirata K, Mizukoshi M, Imanishi T, Akasaka T. Very late clinical cardiac event after BMS implantation: in vivo optical coherence tomography examination. *JACC Cardiovasc Imaging.* 2010;3:525-7.

27. Hou J, Qi H, Zhang M, Ma L, Liu H, Han Z, Meng L, Yang S, Zhang S, Yu B, Jang IK. Development of lipid-rich plaque inside bare metal stent: possible mechanism of late stent thrombosis? An optical coherence tomography study. *Heart.* 2010;96:1187-90.